# Advancing elastic Full Waveform Inversion beyond structural imaging

*Faqi Liu, Guanghui Huang, Cosmin Macesanu, James Sheng, Jaime Ramos-Martínez, Carlos Calderón-Macías and Dan Whitmore, TGS*

**Summary**

We show the power of elastic full waveform inversion (EFWI) beyond deriving a velocity model for depth imaging. Instead, multiparameter elastic FWI (MPEFWI) inverts simultaneously a velocity model and a reflectivity of the subsurface. Application to a narrow azimuth data from offshore Brazil demonstrates that the inverted velocity model produces better depth image and the high resolution reflectivity can be used for quantitative interpretation in reservoir characterization.

**Introduction**

Full Waveform Inversion (FWI) has evolved to a robust and reliable technique to build accurate velocity models for depth imaging which has been routinely applied in seismic processing for both land and marine surveys. By incorporating more accurate physics, elastic FWI further enhances this capability, delivering highly precise models even in structurally complex regions with strong impedance contrasts such as salt boundaries (Macesanu, et al, 2024, Liu, et al, 2025). FWI image or FWI derived reflectivity (FDR), as a directional derivative of a velocity model after high frequency FWI, produces an image with high resolution that is comparable to one from least squares RTM (Wang et al., 2021). Figure 1 show the improved RTM image with significant uplift in salt geometry and subsalt image using a velocity model inverted using dynamic matching elastic FWI (DM EFWI) (Figure 1b) starting with a legacy model as the initial (Figure 1a). The corresponding FWI Image shows the enhanced resolution (Figure 1c).

Traditional single parameter elastic FWI mostly focuses on inverting a P-wave velocity, while shear velocity and density are passively updated following some analytical relation with Vp derived with well constraints. Though this has been proven robust and effective, in geological setting where a class 2p AVO anomaly exists, which is typically localized spatially, density shows opposite trend as P and S wave velocities as shown in Figure 2, a single empirical function can not represent the whole model properly.

By employing a reparameterized elastic wave equation in term of velocity and reflectivity, multiparameter elastic FWI jointly inverts these two independent parameters (Huang, et al, 2025, Macesanu, et al, 2025). This algorithm separates the background velocity and reflectivity effects through a scale separation to the FWI gradients, minimizing the crosstalk during the inversion. More importantly, the new elastic wave equation does not have density explicitly as a parameter, which makes it more favorable to the case described in Figure 2.

Through application to a narrow azimuth data having class 2p AVO anomaly localized in a well, we demonstrate that multiparameter elastic FWI can properly invert the background velocity and reflectivity, from which we can derive a relative density profile that matches nicely with the well log.

**The algorithm**

The multiparameter elastic FWI utilizes the reformulated system of elastic wave equation in term of velocity and reflectivity as follows (Huang *et al*., 2025):

$$\begin{cases} \frac{\partial \tilde{v}_i}{\partial t} = \frac{\partial \sigma_{ij}}{\partial x_j} \\ \frac{\partial \sigma_{ij}}{\partial t} = \tilde{c}_{ijkl}\ \frac{\partial \tilde{v}_k}{\partial x_l} - \tilde{c}_{ijkl}\left(2r_l^p - \frac{1}{V_p}\frac{\partial V_p}{\partial x_l}\right)\tilde{v}_k \end{cases} \quad (1)$$

where $\tilde{v}_i$ $(i = 1,2,3)$ are the weighted particle velocity wavefield; $\sigma_{ij}$ represent the stress tensor, $\tilde{c}_{ijkl}$ are the weighted stiffness tensor, in an isotropic case, they are formulated as

$$\tilde{c}_{ijkl} = \frac{1}{2}\left(V_p^2 - 2V_s^2\right)\delta_{ij}\delta_{kl} + V_s^2\left(\delta_{ik}\delta_{jl} + \delta_{il}\delta_{jk}\right) \quad (2)$$

Which are functions of P and S wave velocity and independent of density. In anisotropic media, they will be functions of Thompsen parameters as well.

In multiparameter elastic FWI, the inversion for velocity and reflectivity are realized by separating the FWI gradient to low and high wavenumber components through a proper imaging condition (Whitmore and Crawley, 2012, Ramos-Martinez *et al*. 2016).

**Application**

Multiparameter elastic FWI was applied to a narrow azimuth streamer dataset acquired in deep-water offshore Brazil. The water depth changes from about 1500 m to over 3000 m with a rugose water bottom. Class 2p AVO anomaly is identified at one of the wells, where, at the reservoir, both sonic and shear logs present increased trend, while the density decreases as shown in Figure 2a-2c. The data was acquired with a narrow azimuth 12-cable configuration separated by 75 m, with a maximum inline offset of 8100 m.

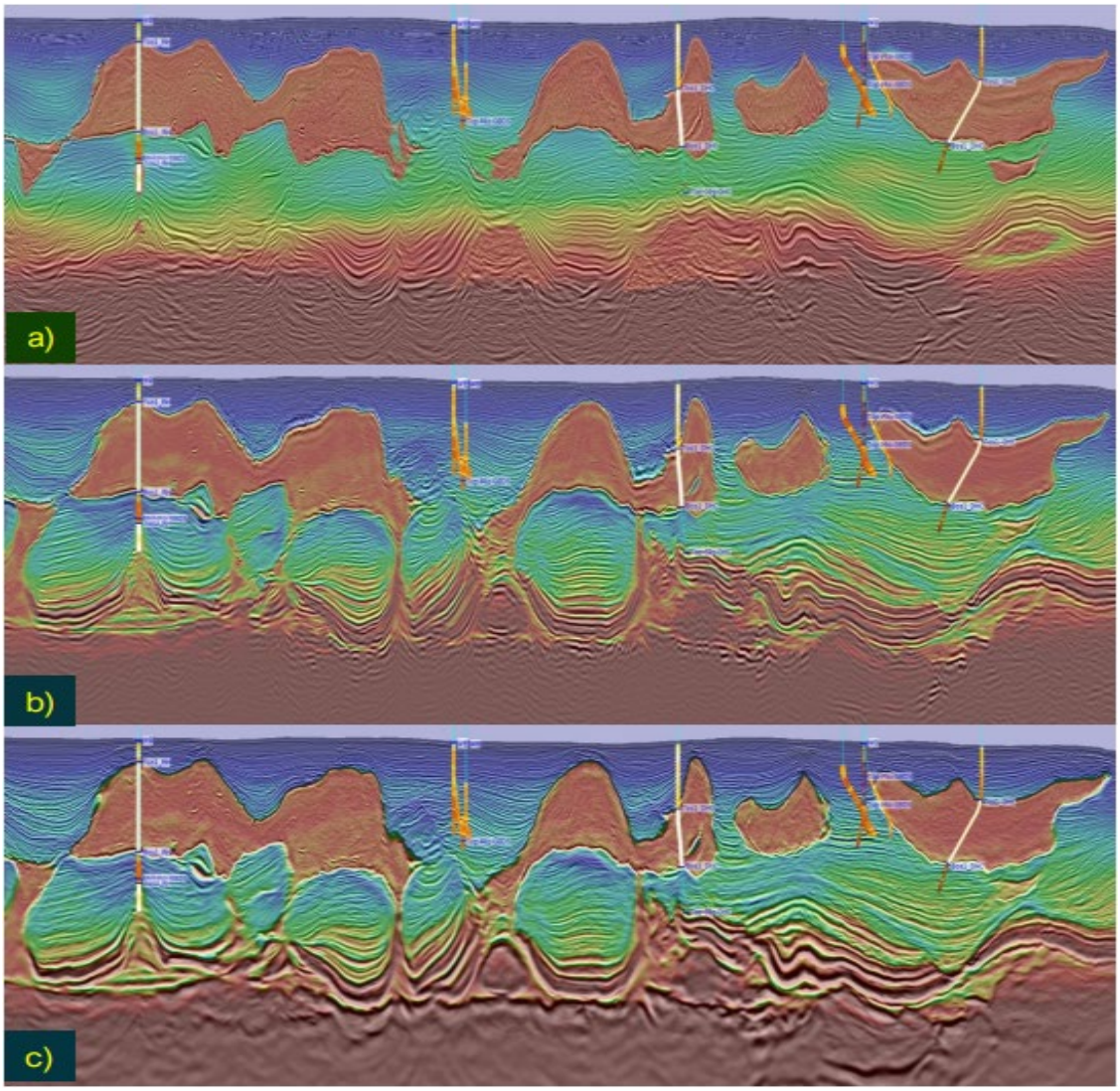

Figure 1: A sparse node example from the Gulf of America: a) RTM image using the legacy model overlaying with it; b) RTM image using EFWI model overlaying the model and c) FWI Image after the EFWI overlaying the model.

Before FWI, the data was applied minimal preprocessing including denoising and debubble. Started from a legacy model as the initial, multiparameter elastic FWI was run staring at 6 Hz and progressively to 35 Hz in 5 different frequency bands to jointly invert the P wave velocity (Vp) and the reflectivity. Figure 3a and 3b show, respectively, the initial velocity model and the corresponding 50 Hz RTM image using this model; Figure 3c and 3d show the inverted velocity model (Vp) and the reflectivity. Due to the scale separation, the inversion produces a low resolution background model, while the high resolution component is in the inverted reflectivity. Compared to the RTM image using the initial model, the inverted reflectivity (Figure 3d) has higher resolution and better focusing as pointed by the arrows. Reflectors below the high-impedance events associated with the presence of volcanic plugs show enhanced continuity and resolution. The inverted velocity (Figure 3c) though low resolution nicely matches with the filtered sonic log (Figure 3e) with more accurate kinematics as evidenced by the improved RTM image shown in Figure 3f compared to that of the initial model in Figure 3b.

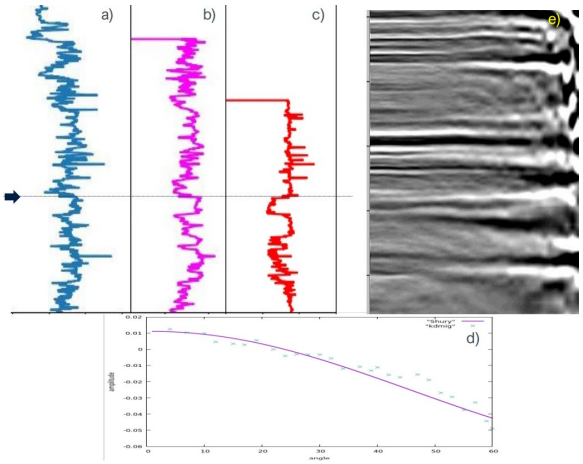


Figure 2: a), b) and c) are the sonic, shear and density log respectively at a well, the arrow points to the depth of the top reservoir where opposite trends occur; d) is the reflection coefficient computed using the model parameters extracted from the logs at the top of the reservoir; e) is a KDMIG common image gather near the well location, the target event at the depth pointed by the arrow shows phase reversal as offset/angle increase, and the amplitude matches the analytical reflection coefficient reasonably well as shown in d).

Starting from the inverted velocity and reflectivity, the impedance and then the density can be derived as shown in Figure 4a), Figure 4b) shows the comparison of the density log (red) against the one derived (blue) from the inverted velocity and reflectivity at the well location as shown in Figure 2. Clearly, the multiparameter elastic FWI overcomes the challenges and successfully represent the case of AVO anomaly.

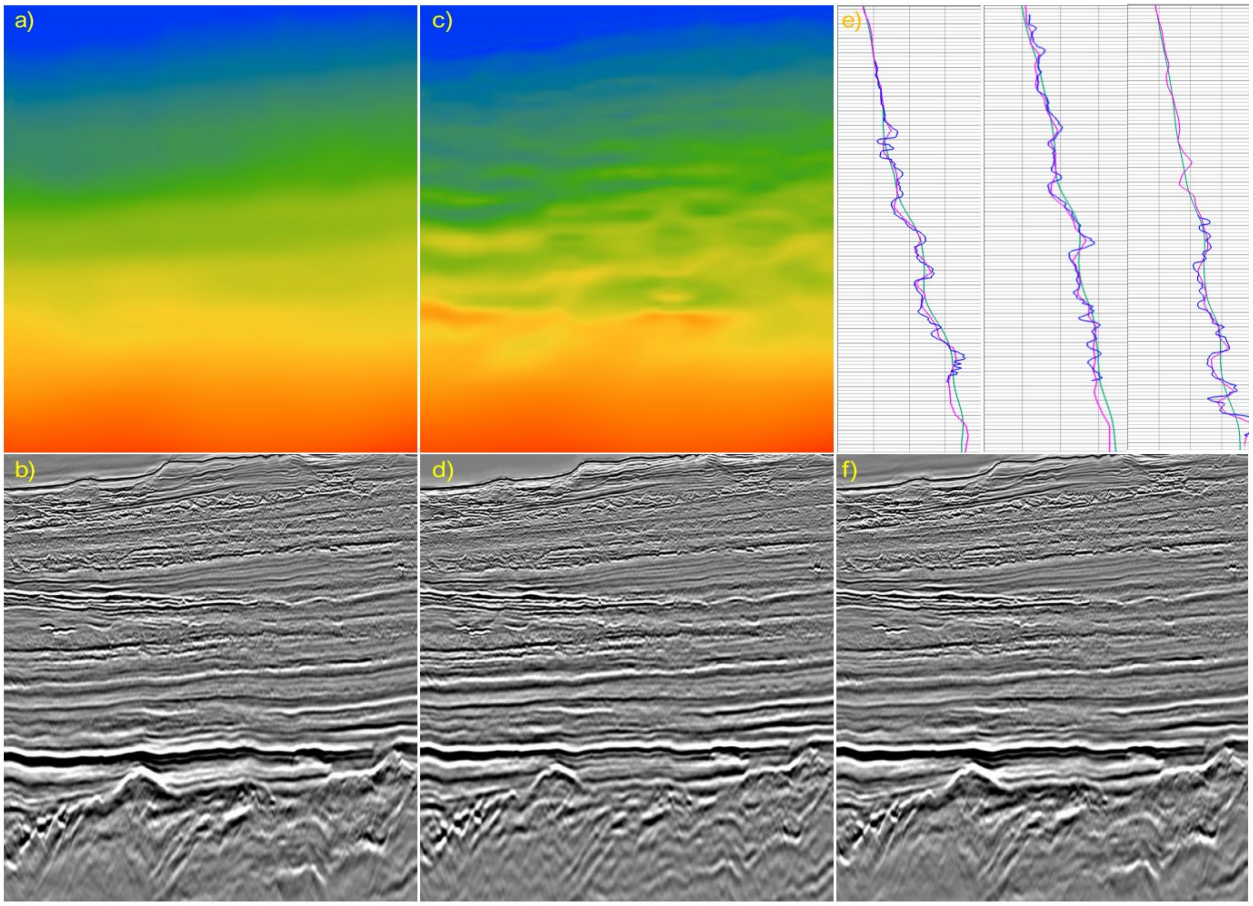


Figure 3: An example from offshore Brazil: a) legacy model used as the initial for the MP EFWI; b) RTM image using the initial model in a); c) Inverted velocity after 35 Hz MP EFWI and d) the inverted reflectivity; e) overlay of filtered sonic log (blue), initial velocity (Green) and the inverted velocity (pink) at 3 well locations; f) RTM image using the inverted velocity in c).

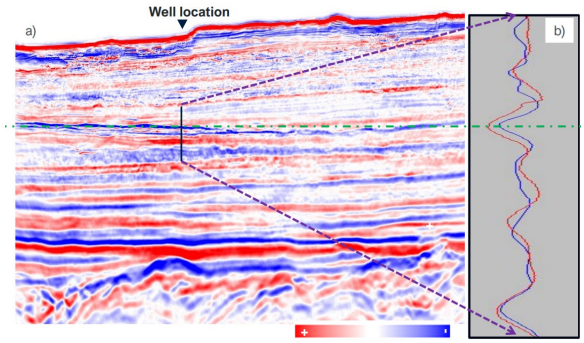


Figure 4: a) Relative density derived from the inverted velocity and reflectivity after MP EFWI; b) the filtered density log (red) comparing to the derived density (blue) at the well where density has opposite trend from velocities as shown in Figure 2. The green line shows the depth of the target reservoir.

**Conclusions**

By leveraging the reformulated system of elastic wave equation, MP EFWI can simultaneously inverts the P-wave velocity and reflectivity in an elastic media, which can be used to derive other properties related to a reservoir. The workflow involves the separation of the FWI gradient to components of different resolution where the low resolution component is used to update the velocity and the high resolution component is to update the reflectivity. This approach effectively mitigates the crosstalk between the parameters. Successful application to a narrow azimuth data demonstrates the robustness of the algorithm.

**Acknowledgements**

We are grateful to our colleagues Hao Xing and Richard Huang for providing the elastic FWI result of the sparse node data, and we thank TGS management for the support and permission to publish this work and TGS Multiclient for the permission to use the data examples.

## References

Huang, G., C. Macesanu, F. Liu, J. Ramos-Martínez, D. Whitmore, and C. Calderón, 2025, Multiparameter elastic FWI for joint inversion of velocity and reflectivity: 86th EAGE Conference & Exhibition, Extended Abstracts.

Liu, F., C. Macesanu, H. Xing, M. Romanenko, G. Zhan, C. Calderón-Macías and B. Wang, 2025, Elastic full-waveform inversion: Enhance imaging for legacy and modern acquisition: The Leading Edge, No.5.

Macesanu, C., G. Huang, F. Liu, J. Ramos-Martínez, and D. Whitmore, 2025, Elastodynamic modeling and inversion with reflectivity terms.

Ramos-Martinez, J., S. Crawley, K. Zou, A.A. Valenciano, L. Qiu, and N. Chemingui, 2016, A robust gradient for long wavelength FWI updates: 78th EAGE Conference & Exhibition, Extended Abstracts.

Wang, B., Y. He, J. Mao, F. Liu, Hao, M. Perz, and S. Mitchel, 2021, Inversion-based imaging: LSRTM to FWI Imaging: First Break, **39**(12), 85-93.

Whitmore, N.D. and S. Crawley, 2012, Applications of RTM inverse scattering imaging conditions: 82nd SEG Annual International Meeting, SEG, Expanded Abstracts, 1-2.